

**THEORETICAL INVESTIGATION OF THE INHIBITION ACTIVITY OF
SOME GINKGO BILOBA FLAVONOIDS DERIVATIVES TOWARD
ACETYLCHOLINESTERASE ENZYMES: MOLECULAR DOCKING AND DFT
APPROACH**

S. Hamdani¹, A. Ghomri^{1,3*}, H. Allali^{1,2}

¹Laboratory of Natural and Bioactives Substances (LASNABIO), Tlemcen, Algeria

²Department of Chemistry, Faculty of Sciences, AbouBekr Belkaïd University, P.O. Box 119,
Tlemcen, Algeria

³High School of Applied Sciences (ESSA), P.O. Box 165, Belhorizon, Tlemcen, Algeria

Received: 10 December 2019 / Accepted: 29 December 2019 / Published online: 01 January 2020

ABSTRACT

Inhibition of acetylcholinesterase (AChE) presents a key for the treatment of Alzheimer's disease (AD), an important number of natural inhibitors of this enzyme have been studied. *Ginkgo biloba* extracts were used as a treatment of AD. In this work, we present a theoretical study of AChE enzyme (pdb code 1hbj) inhibitors by flavonoids derived from *Ginkgo biloba* extracts using molecular Docking and conceptual DFT methods. Theoretical calculations of flavonoids interactions with AChE were performed using Molecular Operating Environment (MOE) software. Obtained results show that the natural molecules extracted from *Ginkgo biloba* present a good inhibitor of AChE, our results explain also the interaction mechanism. We note that Kaempferol-3-*O*-glucopyranoside present the most active system in our series showing the best interaction energy and the most important descriptors values, our obtained results are in good agreement with the IC₅₀ values obtained experimentally.

Keywords: Molecular docking; Alzheimer's disease; *Ginkgo biloba*; Flavonoids.

Author Correspondence, e-mail: ghomriamina@yahoo.fr

doi: <http://dx.doi.org/10.4314/jfas.v12i1S.25>



1. INTRODUCTION

Alzheimer's disease (AD) is a neurodegenerative disease that especially affects older people [1]. AD is relentless; to date there is no effectient treatment that breaks the AD progression [2]. An important number of studies on several medicinal plants have been carried out and have shown their effectiveness as a therapy for AD, the most known are *Ginseng* extracts [3], *Celastrus paniculatus* seeds [4,5] and *Curcuma longariz* homes [6,7]. *Ginkgo bilobawas* used in the treatment of cognitive dysfunctions and have proven a good efficiency [8]. *G.bilobaleaves* have been used since early times to treat neurodegenerative diseases such as AD [9] andalso presented antioxidant [10], anti-inflammatory [11], neuroprotective [12] and anti-aging [13] properties.

Our aim in this study is to elucidate theoretically the acetylcholinesterase (AChE) inhibition activity by a series of natural inhibitors extracted from *G. biloba* using molecular modeling methods namely molecular docking [14] and conceptual density functional theory (DFT) derived reactivity indices [15]. In addition, the solvent effect solvent on the interaction between the enzyme and the best inhibitor was also treated, on the other hand DFT derived reactivity indices were calculated for the best inhibitors aiming to verify the correlation probability between the biological activity and the molecular reactivities. The selected natural inhibitors [16-18] are given in Table 1. Our, results will contribute in the designof new active molecules as AChE inhibitors, that can be synthetized basing on the molecular structures of bioactive compounds of *G. biloba*.

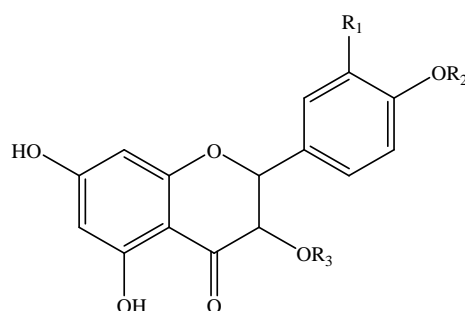
Table 1. Molecules treated in our study

Compounds	Name	IUPAC name	PubChem CID	Molecular Formula	IC ₅₀ (μM)	Ref
1	Quercetin	2-(3,4-dihydroxyphenyl)-3,5,7-trihydroxychromen-4-one.	5280343	C ₁₅ H ₁₀ O ₇	316.97	[16]
2	Kaempferol	3,5,7-trihydroxy-2-(4-hydroxyphenyl)chromen-4-one.	5280863	C ₁₅ H ₁₀ O ₆	352.35	[16]
3	Taxifolin	(2R,3R)-2-(3,4-dihydroxyphenyl)-3,5,7-trihydroxy-2,3-dihydrochromen-4-one.	439533	C ₁₅ H ₁₂ O ₇	437.47	[16]
4	Ermanin	5,7-dihydroxy-3-methoxy-2-(4-methoxyphenyl) chromen-4-one.	5352001	C ₁₇ H ₁₄ O ₆	281.59	[16]
5	Quercetin-3-O- -D-glucopyranoside	2-(3,4-dihydroxyphenyl)-5,7-dihydroxy-3-[(2S,3R,4S,5S,6R)-3,4,5-trihydroxy-6-(hydroxymethyl)oxan-2-yl]oxychromen-4-one.	5280804	C ₂₁ H ₂₀ O ₁₂	124.47	[16]
6	Quercetin-3-O- -D-glucopyranoside	2-(3,4-dihydroxyphenyl)-5,7-dihydroxy-3-(((2S,3S,4R,5R,6S)-3,4,5-trihydroxy-6-(hydroxymethyl)oxan-2-yl)oxy)chromen-4-one.	/	C ₂₁ H ₂₀ O ₁₂	170.98	[16]
7	Kaempferol-3-O-glucopyranoside	5,7-dihydroxy-2-(4-hydroxyphenyl)-3-[(2S,3R,4S,5S,6R)-3,4,5-trihydroxy-6-(hydroxymethyl)oxan-2-yl]oxychromen-4-one.	5282102	C ₂₁ H ₂₀ O ₁₁	80.40	[17]
8	Quercetin-3-O-galactoside	2-(3,4-dihydroxyphenyl)-5,7-dihydroxy-3-[(2S,3R,4S,5R,6R)-3,4,5-trihydroxy-6-(hydroxymethyl)oxan-2-yl]oxychromen-4-one.	5281643	C ₂₁ H ₂₀ O ₁₂	142.12	[18]
9	Quercetin-3-O- -L-rha-(1 2) - -D-glucopyranoside	3-(((2R,3S,4S,5S,6R)-4,5-dihydroxy-6-methyl-3-(((2R,3S,4R,5R,6S)-3,4,5-trihydroxy-6-(hydroxymethyl)tetrahydro-2H-pyran-2-yl)oxy)tetrahydro-2H-pyran-2-yl)oxy)-2-(3,4-dihydroxyphenyl)-5,7-dihydroxy-4H-chromen-4-one.	/	C ₂₇ H ₃₀ O ₁₆	126.94	[16]

2. MATERIALS AND METHODS

The enzyme structure was downloaded from the Protein Data Bank archive-information database (www.rcsb.org/pdb) (code 1hbj) [19] with a three-dimensional structure obtained by

X-ray diffraction (resolution 2.5Å). According to recent research, the flavonoids used in our work have been identified, and their molecular structures (Fig.1) have been present edusing the ChemDraw software. The physico-chemical properties of the ligands are reported in Table 2. Lipinski's rule [20] which is a valuable tool for selecting the good candidates by predicting drug-like properties was also verified for all our ligands. AChE enzyme is presented in (Fig.2) with 1539 residues. Enzyme and ligand energies minimization and the active site identification were performed using MOE (Molecular Operating Environment) software [21].



Lig	R ₁	R ₂	R ₃
1	OH	H	H
2	H	H	H
4	CH ₃	H	CH ₃
5	OH	H	CH ₃ u β-Gl
6	OH	H	β-Glu α-Glu
7	H	H	α-Glu β-Gl
8	OH	H	β-Glu β-Glu
9	OH	H	Rha-(1 2)-Glu-

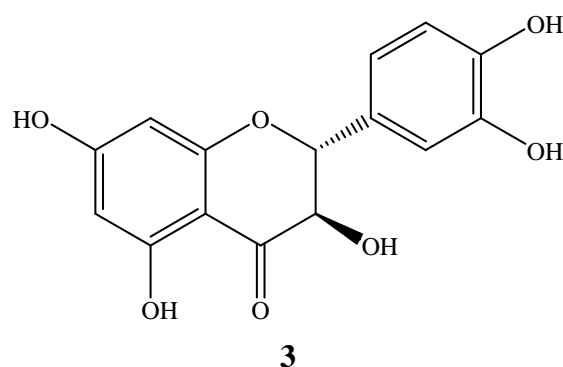


Fig.1. Ligands corresponding structures

Energy minimization was performed under the following conditions: temperature = 300 °K, pH = 7, geometry minimization was done using the Mmff94x [22] force field implanted in MOE program and AM1 [23] Hamiltonian. In Figure 3 the enzyme active site with the co-crystallisation molecule is presented, the minimised energies of the ligands and their toxicities are given in Table 2.

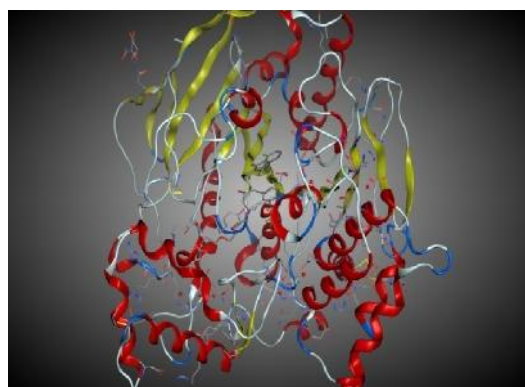


Fig.2. Simplified model of enzyme 1hbj.

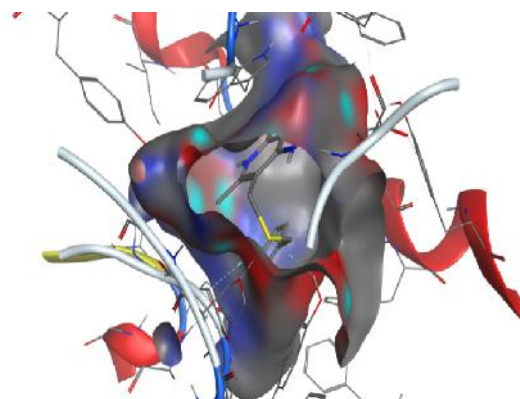


Fig.3. Active site enzyme isolated.

Table 2. Ligands properties

N/ Ligand	Weight	TPSA	LogP	LogS	H-bonds donors	H-bonds acceptors	Toxicity
1	302.24	127.45	2.01	-2.77	5	6	NO
2	285.23	110.05	2.74	-3.40	3	5	NO
3	304.25	127.45	1.28	-2.01	5	7	NO
4	314.29	85.22	2.70	-3.96	2	5	NO
5	464.38	206.60	-0.73	-2.55	8	11	NO
6	464.38	206.60	-0.73	-2.55	8	11	NO
7	447.37	189.20	0.00	-3.17	6	10	NO
8	464.38	206.60	-0.73	-2.55	8	11	NO
9	610.52	265.52	-1.88	-2.79	10	15	NO

Weight: Molecular weight (g/mol), TPSA: Polar surface area (\AA^2), logP: Octanol-water partition coefficient, logS: aqueous solubility, H- bonds donors: Number of H- bonds donors, H- bonds acceptors: Number of H- bonds acceptors.

The above table reflects the fact that our ligands are non-toxic and can present biological activities.

3. RESULTS AND DISCUSSION

3.1 Molecular docking

The molecular docking results and the interactions of the 3 best inhibitors ligands are shown in Table 3 and Figures 4.a, b; 5.a, b and 6.a, b.

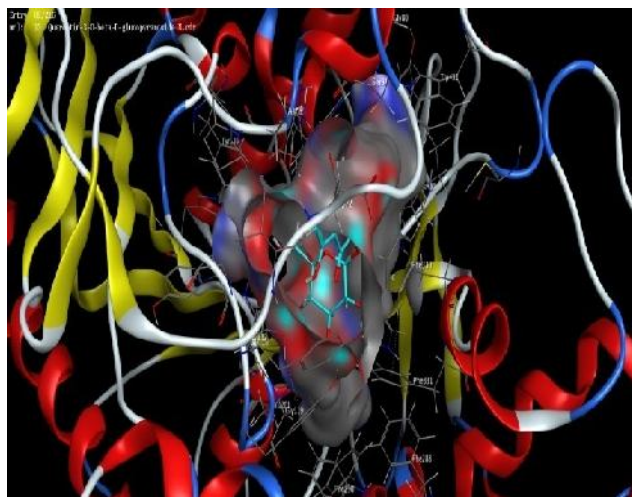


Fig.4.a. Diagram of interactions (Enzyme/ligand)

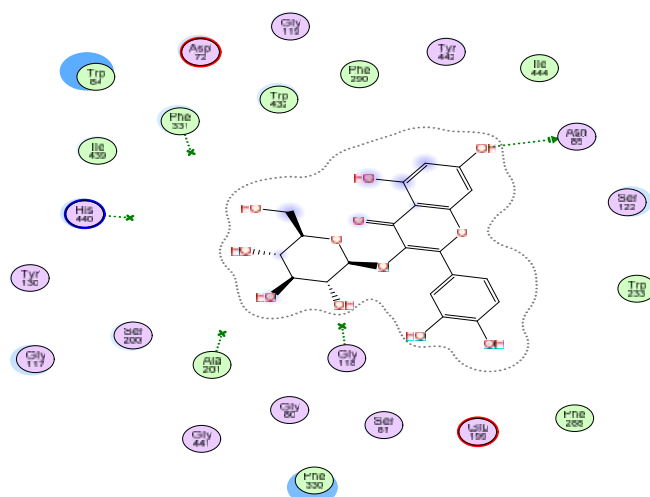


Fig.4.b. Diagram interaction of complex-5(1hbj + Quercetin-3-O- -D-glucopyranoside)

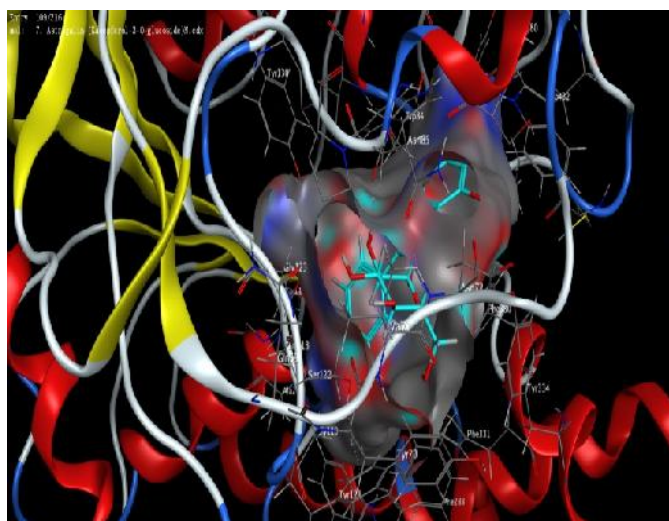


Fig.5.a. Diagram of interactions (Enzyme/ligand)

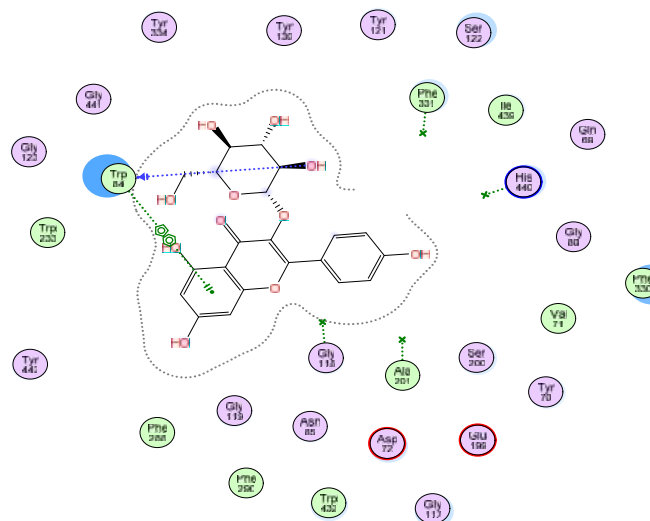


Fig.5.b. Diagram interaction of complex-7(1hbj + Kaempferol-3-O-glucopyranoside)

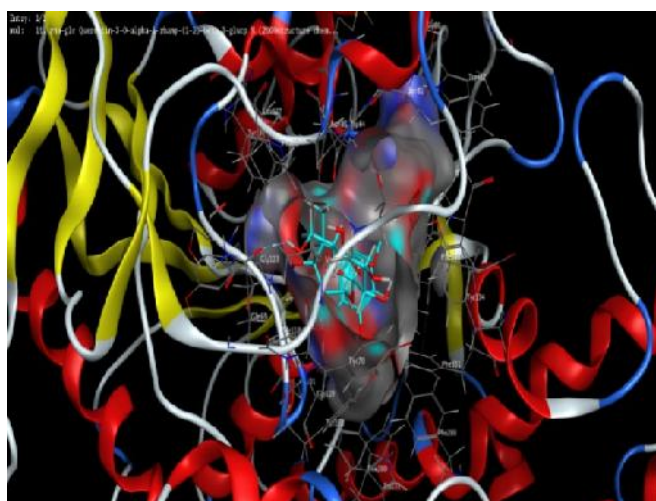


Fig.6.a.Diagram of interactions (Enzyme/ligand)

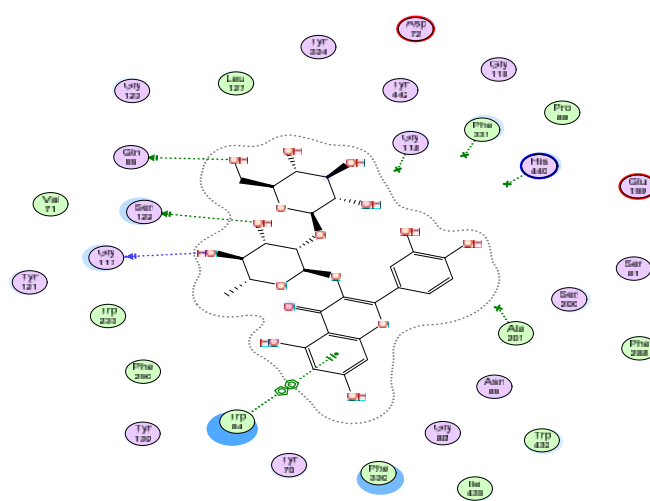


Fig.6.b. Diagram interaction of complex-9 (1hbj+Quercetin-3-O- -L-rhamnopyranosyl-(1 2)- -D-glucopyranoside)

Table 3. Energy Balance of 9Complexes (AChE/ligand) (Kcal/mol)

Lig	Score	Rmsd-Refine	E-Conf	E-Place	E-Score1	E-Refine	E-Score2	TRD-Score
Lig-Ref	-7.1231	1.6423	131.9414	-49.6395	-13.2266	-8.7118	-7.1231	/
Complex-1	-6.4512	1.7002	34.2665	-93.7788	-14.6746	-23.4841	-6.4512	8
Complex-2	-6.4511	0.7477	35.8478	-114.6268	-13.3696	-20.6032	-6.4511	9
Complex-3	-6.3749	2.1422	51.4140	-74.8596	-13.7208	-22.8995	-6.3749	10
Complex-4	-7.3361	2.1074	68.5911	-68.5265	-13.9923	-22.0186	-7.3361	7
Complex-5	-8.6472	3.2457	135.9885	-108.3850	-16.1367	-16.0136	-8.6472	2
Complex-6	-8.0825	0.8319	156.2376	-159.9268	-18.0761	-18.0201	-8.0825	5
Complex-7	-8.8359	1.9417	132.0856	-124.5178	-15.6647	-25.5160	-8.8359	1
Complex-8	-8.1182	1.5049	146.3952	-80.5852	-14.2365	-17.0717	-8.1182	4
Complex-9	-8.4217	1.4222	227.5072	-136.6125	-17.1755	0.3644	-8.4217	3

S: the final score; *is* the score of the last step, *rmsd_refine*: the mean square deviation between the laying before refinement and after refinement pose, *E_conf*: energy conformer, *E_place*: score of the placement phase, *E_scor1*: score the first step of notation, *E_refine*: score refinement step and number of conformations generated by ligand *E_scor2*: score the first step notation; *Trd-score*: is the score trends.

Table 3 and Figure 5 show that ligand orientation plays an important role in the active site ligand positioning. We note, that the introduction of large groups causes a rearrangement of the conformation inside the active site cavity. Residues are marked with their 3-letter code and

classification. The complexes energy balances are presented in Table 3. In this work, we focused on the interactions of the highest scoring complex. For the protocol validation, the obtained result shows that the RMSD ≤ 2 which means that our Docking protocol is valid. The results in Table 3 show that the complex formed with Kaempferol-3-*O*-glucopyranoside gives the highest score (-8.8359 Kcal/mol), i.e. the most stable complex. The second stable complex is given with the Quercetin-3-*O*- β -D-glucopyranoside ligand (-8.6472 Kcal/mol). The third important score is given by Quercetin-3-*O*- β -L-rhamnopyranosyl-(1 \rightarrow 2)- β -D-glucopyranoside (-8.4217 Kcal/mol).

Basing on the obtained results, we conclude that the reference ligand (Lig-Ref) interacts with amino acids [GLY 118 (A) by an H acceptor, ALA 201 (A) by an H acceptor, HIS 440 (A) by an H-pi type interaction; PHE 331 (A) by pi-H] at a distances of 3.79; 2.69; 4.32; 3.76(Å) and by an energies between (-2.5 and -0.6) kcal/mol.

The complex formed with Kaempferol-3-*O*-glucopyranoside is the most stable (Fig.5.a, b), for which it forms two interactions with the amino acid [TRP 84 (A) with an H-donor and TRP 84 (A) with a pi-pi interaction] with distances of 2.95; 3.74Å and energies of -1.9 and -0.0 kcal/mol respectively.

For complex 5 (Fig.4.a, b): Quercetin-3-*O*- β -D-glucopyranoside interacts with the amino acid ASN 85 (A) via an H-donor at a distance of 3.03Å and an energy of -0.7 kcal/mol; finally for complex 9 (Fig.6.a,b): Quercetin-3-*O*- β -L-rhamnopyranosyl-(1 \rightarrow 2)- β -D-glucopyranoside interacts with amino acid [GLN 69 (A) by H-donor, GLY 117 (A) by H-donor, SER 122 (A) by H-donor and TRP 84 (A) with pi-pi interaction] the respective distances were 2.61 ; 2.76; 2.51; 3.79 Å and at energies between (-2.9 and -0.0) kcal/mol.

For a best interpretation of our results, we compared the obtained docking scores with the experimentally obtained activities (IC₅₀ values). Results are shown in Table 4:

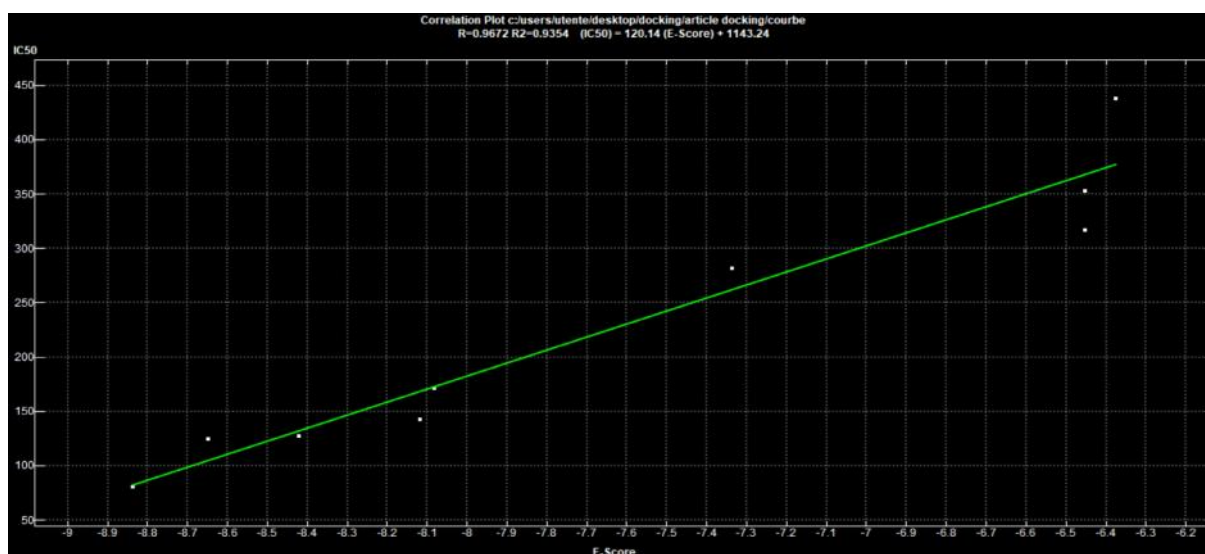
Table 4. Comparison between IC₅₀ and docking score

Compounds	IC ₅₀ (μ M)	Trd-IC ₅₀	Trd-Score
1	316.97	7	7
2	352.35	8	8
3	437.47	9	9
4	281.59	6	6
5	124.47	2	2
6	170.98	5	5
7	80.40	1	1
8	142.12	4	4
9	126.94	3	3

Table 4 shows that the scores obtained trends is the same as the experimentally obtained IC₅₀ trend. Indeed, the experimental activities of the ligands are classified as follows:

Lig7>Lig5>Lig9>Lig8>Lig6>Lig4>Lig1>Lig2>Lig3, this same order is obtained by our calculations:Lig7(-8.8359)>Lig5(-8.6472)>Lig9(-8.4217)>Lig8(-8.1182)>Lig6(-8.0825)>Lig4(-7.3361)>Lig1(-6.4512)>Lig2(-6.4511)>Lig3(-6.3749) which justifies that our results are in very good agreement with the experimental outcomes.

The following curve represents well that our scores correlate very well with the experimental IC₅₀.

**Fig.7.** Correlation plot (Docking obtained scores) X axis, (experimental IC₅₀) Y axis

We conclude that there is a very good correlation between the obtained scores and the IC_{50} values with a correlation coefficient of 0.9354 which is considered as excellent.

3.2 Solvation effect on the complexes stabilities study

It should be noted that the water presence is important to ensure a good interaction between the ligand and the active site. Furthermore, the calculation in the presence of water reflects more the reality so the behaviour of the water molecules in direct contact with the solute is very important. Figures 8, 9 (a, b), 10 (a, b), 11 (a, b) and 12 show the schematics, interaction diagrams and graphic legend of the complex (enzyme/Ligand) in water.

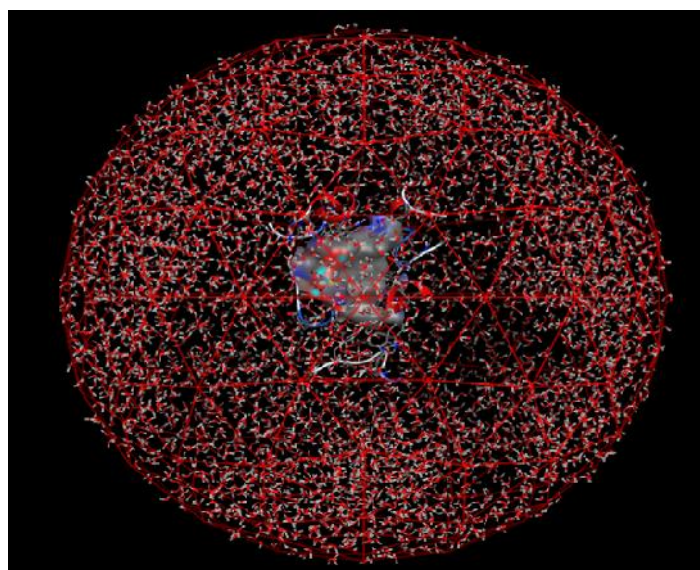


Fig.8. Solvations Ligand-enzyme in elliptical box

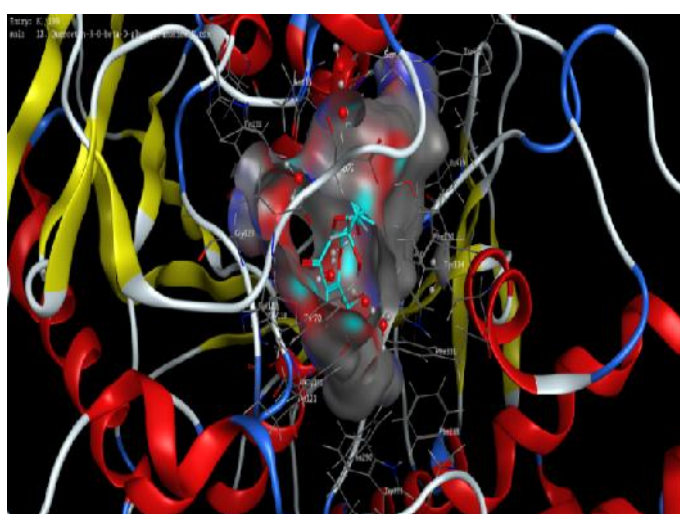


Fig. 9.a. Diagram of interactions (Enzyme/ligand) in water

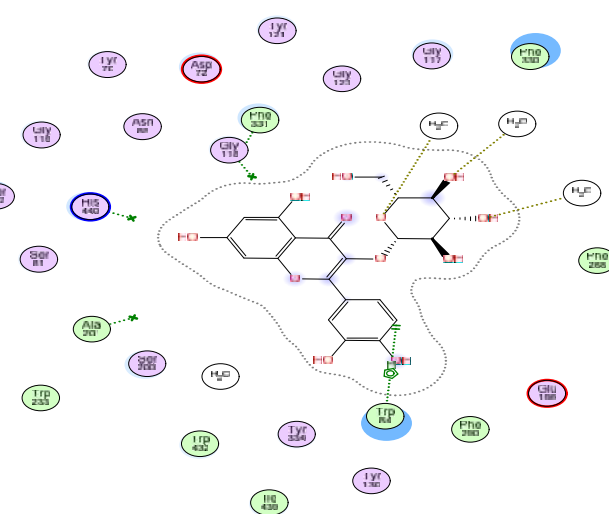


Fig. 9.b. Diagram interaction of complex-5 (1hbj + Quercetin-3-O-D-glucopyranoside)

It turn out from the previous figures and Table 5 that the formed complex (AChE/Lig7) in water represents the best score (-7.3901 Kcal/mol) compared with ligands 5 and 9 and the diagram of the complex formed shows that its interactions are made with amino acids[GLU 199 (A) H-donor type interaction; ASP 72 (A) also H-donortype and TRP 84 (A) pi-pi interaction] at distances of 2.84; 3.12; 3.92 Å and energies that vary between (-3.4 and -0.0) kcal/mol (Fig.10.a, b).

Lig-Ref interacts with amino acid[HOH 0 donor-H type; GLY 118 (A) acceptor H type; ALA 201 (A) also with an acceptor H; HIS 440 (A) with an interaction of H-pi type and PHE 331 (A) by an interaction pi-H] at distances of 3.14; 3.79; 2.69; 4.32; 3.76 Å respectively and at an energy between (-2.5 and -0.5) kcal/mol.

For complex 5 (Fig.9.a,b): Quercetin-3-*O*- β -D-glucopyranoside interacts with amino acids[HOH 0 with an H-donor; HOH 0 with an H-acceptor; HOH 0 also with an H-acceptor; TRP 84 (A) with an H-pi interaction at distances of 2.56; 2.54; 2.57; 3.43 Å and energies between (-0.7 and 2.0) kcal/mol.

For complex 9 (Fig.11.a,b): Quercetin-3-*O*- β -L-rhamnopyranosyl-(1 \rightarrow 2)- β -D-glucopyranoside interacts with amino acids[HOH 0 by an H-donor ; HIS 440 (A) by an H-donor ; SER 122 (A) also by an H-donor ; PHE 330 (A) by pi-pi interaction at distances of 2.74; 2.85; 2.74; 3.59 Å and energies between (-2.9 and -4.9) kcal/mol.

The graphical legend of the 2D interaction is shown in Figure 12.

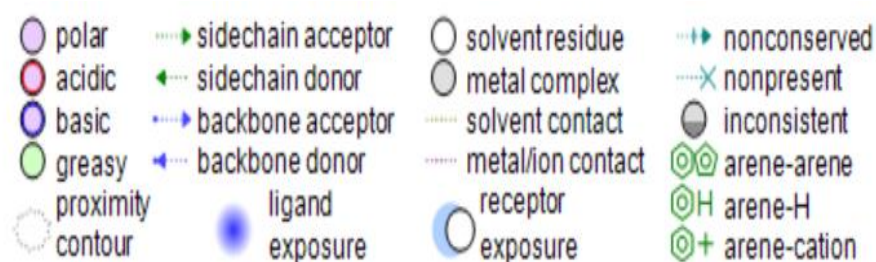


Fig.12. 2D graphical legend

3.3 DFT derived reactivity indices

The relative reactivities of the most active ligands (Lig 7, Lig 5 and Lig 9) and the reference ligand were elucidated through the DFT derived reactivity indices, obtained results are given in Table 6.

Table 6. HOMO and LUMO energies, and global reactivity indices μ , χ , n max, Nu for Lig-Ref, Lig5, Lig7 and Lig9

Compounds	HOMO (au)	LUMO(au)	μ (au)	χ (ev)	n max	Nu(ev)
Lig-Ref	8.497	0.614	-3.94	23.20	0.43	22.18
Lig5	-9.261	0.763	-4.25	24.50	0.42	35.61
Lig7	-9.326	-1.903	-5.61	57.77	0.76	33.82
Lig9	-7.898	0.756	-3.57	20.05	0.41	73.24

Obtained results show that, for the three ligands the trends of the maximum charge transfer as well as the global electrophilicity values is the same that the trend of the experimental IC_{50} . Indeed, for the electrophilicity ligand 7 presents the most electrophilic power (χ (Lig7) = 57.77 eV) followed by ligand 5 (χ = 24.50 eV) and the Ligand 9 presents the lowest electrophilic power with a value of χ (Lig9) = 20.05 eV; this order shows that the biological activities of these ligands is directly related to their reactivities and that the more electrophilic ligand is the more active one. On the other hand, Table 6 also shows that the global nucleophilicity and electronic chemical potential of ligands correlate inversely with biological activities, as per our results show that ligand 7 is the least nucleophilic ligand and also the one that represents the lowest value of electronic chemical potential. It should be noted that the results obtained with the conceptual DFT are in very good agreement with the experimental results and also with the scores obtained with molecular docking.

6. CONCLUSION

In this work, we studied the inhibition of AChE by flavonoids extracted from *G. biloba*, using molecular modelling methods including molecular docking and DFT derived reactivity indices, the solvent effect was also elucidated in our study. Our calculations show that inhibitor 7 (Kaempferol-3-O-glucopyranoside) has a more improved enzyme inhibition followed by inhibitors 5 and 9. The interactions between the enzyme and these inhibitors are of different types H-acceptors, H-donors, H-pi, pi-H, pi-pi, HOH π with an H-donor and HOH π with an H-acceptor. The solvation model involving the coordination of solvent molecules with the

interacting (complex) system shows a remarkable influence of the solvent on the interaction energies and consequently the influence of the solvent type on the inhibitory activity. Our results also show that the conceptual DFT derived reactivity indices provide a good tool for the biological activities study and can represent very good descriptors for performing predictive models of biological activities. Indeed, in our study we found that global electrophilicities as well as global charge transfers are directly related to activities, and the global nucleophilicities and electronic chemical potentials that are inversely related to activities. In conclusion our results are in very good agreement with the experimental results and therefore our ligands can present the basic skeleton for the design of a treatment for AD.

7. ACKNOWLEDGEMENTS

Authors thanks the Algerian Ministry of Higher Education and Scientific Research for the support under the PRFU project (approval No: B00L01EP130220190002), Authors thanks also Mr MISSOUM Nouredine member of the laboratory of Natural and Bioactive Substances Tlemcen University, Algeria.

8. REFERENCES

- [1] Singhal AK, Naithani V, Bangar OP. Medicinal plants with a potential to treat Alzheimer and associated symptoms. *Int. J.Nutr. Pharmacol. Neurol. Dis.*, 2012, 2: 84-91.
- [2] Zhang L, Li D, Cao F, Xiao W, Zhao L, Ding G and Wang ZZ. Identification of Human Acetylcholinesterase Inhibitors from the Constituents of EGb761 by Modeling Docking and Molecular Dynamics Simulations. *Comb. Chem. High Throughput Screen.*, 2018, 21:41-49.
- [3] Sunoh K, Taehyun K, Kwangseog A, Woo-Kyu P, Seung-Yeol N, Hyewhon Rhim. *Biochem. Biophys. Res. Commun.*, 2004, 323: 416-424. doi: 10.1016/j.bbrc.2004.08.106
- [4] Alama B, Haque E. Anti-Alzheimer and Antioxidant Activity of *Celastrus paniculatus* Seed. 2011, 7(1):49-56.
- [5] Kumar MHV, Gupta YK. *Phytomedicine*. 2002, 9 (1): 302-311. doi: 10.1078/0944-7113-00136
- [6] Miquel J, Bernd A, Sempere J M, Diaz-Alperi J, Ramirez. *Arch. Gerontol. Geriatr.*, 2002, 34:37-46. doi: 10.1016/S0167-4943(01)00194-7

- [7] Mishra S, Palanivelu K. Ann. Indian Acad. Neurol., 2008, 11(1): 13-19. doi:10.4103/0972-2327.40220
- [8] Loew D. Value of *Ginkgo biloba* in treatment of Alzheimer dementia. Wien Med. Wochenschr., 2002, 152 (15-16): 418-422.
- [9] Ramassamy C, Longpré F, Christen Y, *Ginkgo biloba* extract (EGb 761) in Alzheimer's disease: is there any evidence. Curr. Alzheimer Res., 2007, 4(3): 253-262.
- [10] Droy-Lefaix MT. Age (Omaha). 1997, 20(3): 141-9. doi:10.1007/s11357-997-0013-1
- [11] Kaur S, Sharma N, Nehru B. Inflammopharmacology, 2018, 26(1):87-104. doi:10.1007/s10787-017-0396-2
- [12] Smith PF, MacLennan K, Darlington CL. The neuroprotective properties of the *Ginkgo biloba* leaf: a review of the possible relationship to platelet-activating factor (PAF). J. Ethnopharmacol., 1996, 50(3):131-139.
- [13] Shi C, Xiao S, Liu J, Guo K, Wu F, Yew DT, Xu J. Platelets. 2010, 21(5):373-9. doi:10.3109/09537100903511448
- [14] Huang N, Shoichet BK, Irwin JJ. Benchmarking sets for molecular docking. J. Med. Chem., 2006, 49(23):6789-6801.
- [15] Ghomri, A, Mekelleche S M. Reactivity and regioselectivity of five-membered heterocycles in electrophilic aromatic substitution: A theoretical investigation. J. Mol. Struct. THEOCHEM., 2010, 941(1-3):36-40.
- [16] Xiao Ding, Ming-An Ouyang, Xiang Liu and Rei-Zhen Wang. Acetylcholinesterase Inhibitory Activities of Flavonoids from the Leaves of *Ginkgo biloba* against Brown Planthopper. J. Chem., 2013, Article ID 645086, 4 pages, 2013. <https://doi.org/10.1155/2013/645086>.
- [17] Mira A, Yamashita S, Katakura Y and Shimizu K. J. Molecules. 20, 2015, 4813-4832, doi:10.3390/molecules20034813
- [18] Hernandez MF, Falé PLV, Araujo MEM, Serralheiro MLM. Acetylcholinesterase inhibition and antioxydant activity of the water extracts of several *Hypericum* species. J. Chem., 2010, 120:1076-1082.
- [19] The Protein Data Bank H.M. Berman, J. Westbrook, Z. Feng, G. Gilliland, T.N. Bhat, H. Weissig, I.N. Shindyalov, P.E. Bourne (2000) Nucleic Acids Research, 28:235-242. doi:10.1093/nar/28.1.235

[20] Lipinski CA, Lombardo F, Dominy BW, Feeney PJ. Adv. Drug Deliv. Rev., 2001, 46 (1-3):3-26. doi:10.1016/S0169-409X(00)00129-0.

[21] Chemical Computing Group, Scientific Vector Language, www.chemcomp.com/MOE-Molecular, 2018.

[22] Thomas AH. Merck Molecular force field. I. Basis, form, scope, parameterization, and performance of MMFF94. J. Comput. Chem., 1996, 17:490-519.

[23] Dewar MJS, Zoebisch EG, Healy EF, Stewart JJP. Journal of the American Chemical Society. 1985, 107 (13), 3902. doi:10.1021/ja00299a02.

How to cite this article:

Hamdani S, Ghomri A and Allali H. Theoretical investigation of the inhibition activity of some *ginkgo biloba* flavonoids derivatives toward acetylcholinesterase enzymes: molecular docking and dft approache. J. Fundam. Appl. Sci., 2020, 12(1S), 347-362.